journal

J. Am. Ceram. Soc., **81** [1] 225–28 (1998)

Contact Damage Accumulation in Ti_3SiC_2

It Meng Low,[†] Seung Kun Lee,[*,‡] and Brian R. Lawn[*]

Materials Science and Engineering Laboratory, National Institute of Standards and Technology, Gaithersburg, Maryland 20899

Michel W. Barsoum[*]

Department of Materials Engineering, Drexel University, Philadelphia, Pennsylvania 19104

The evolution of deformation–microfracture damage below Hertzian contacts in a coarse-grain Ti_3SiC_2 is studied. The Hertzian indentation stress–strain response deviates strongly from linearity beyond a well-defined maximum, with pronounced strain–softening, indicating exceptional deformability in this otherwise (elastically) stiff ceramic. Surface and subsurface ceramographic observations reveal extensive quasi-plastic microdamage zones at the contact sites. These damage zones are made up of multiple intragrain slip and intergrain shear failures, with attendant microfracture at high strains. No ring cracks or other macroscopic cracks are observed on or below the indented surfaces. The results suggest that Ti_3SiC_2 may be ideally suited to contact applications where high strains and energy absorption prior to failure are required.

I. Introduction

RECENTLY, dense polycrystalline Ti_3SiC_2 has been developed by reactively hot-pressing Ti, SiC, and C (graphite) powders.[1] Ti_3SiC_2 has a hexagonal crystallographic structure with planar Si layers linked by TiC octahedra, and with weakly bonded basal slip planes.[2] This material displays a unique combination of properties.[3] It is oxidation resistant, and possesses high electrical and thermal conductivity. It has a high elastic modulus ($E \approx 320$ GPa) but a low hardness ($H \approx 4$ GPa), and is machinable. The value $H/E = 0.013$ is exceptionally small for a ceramic,[4] more reminiscent of soft metals. In Vickers indentation tests a multiplicity of energy-absorbing deformation mechanisms operate, predominantly basal slip but also grain buckling as well as grain sliding.[3]

In this communication we investigate the contact deformation of Ti_3SiC_2 using Hertzian indentation.[5,6] Indentation stress–strain data reveal exceptional quasi-plasticity in this material, with a pronounced strain–softening ''tail.'' Ceramographic sectioning is used to examine the nature of the subsurface quasi-plastic damage. Our experiments confirm shear–activated basal slip deformation within grains as the key to the exceptional high quasi-plasticity.

II. Experimental Procedure

Details to the powder processing and ensuing microstructure of Ti_3SiC_2 have been presented elsewhere.[1] Polycrystalline specimens were fabricated by weighing stoichiometric proportions of Ti (99.3% pure, 325 mesh, Titanium Specialists, Sandy, UT), SiC (99.7% pure, mean particle size 4 μm, Atlantic Equipment Engineers, Bergenfield, NJ), and C (99% pure, mean particle size 1 μm, Aldrich, Milwaukee, WI) powders, mixing in a V-blender for 2 h, and reactive hot pressing at 1600°C for 4 h under a pressure of 40 MPa. The microstructure of the sintered material investigated here consists of large platelike grains of diameter 50–200 μm and thickness 5–20 μm, with a heavily striated texture.[1,3] All test surfaces were diamond-polished to 1 μm finish.

Vickers indentations were made at $P = 1$–1000 N to measure hardness, determined here as $H = P/2a^2$, where P is peak load and a is impression half-diagonal.

Hertzian indentations were made using tungsten carbide (WC) spheres of radius $r = 1.21$–12.7 mm, at peak loads up to $P = 4000$ N. Measurements of contact radius a (made visible by first coating the specimen surface with a gold film) at each given load P and sphere radius r enabled calculation of indentation stresses, $p_0 = P/\pi a^2$, and indentation strains, a/r, for construction of an indentation stress–strain curve.[5,7] An indentation yield stress $p_0 = p_Y$ was evaluated from the threshold loads above which permanent impressions were first detected on the contact surface.[8]

Bonded-interface specimens were used to provide sections of the Hertzian contact damage.[5,7] These specimens were prepared by bonding together two polished half-blocks 30 mm ×

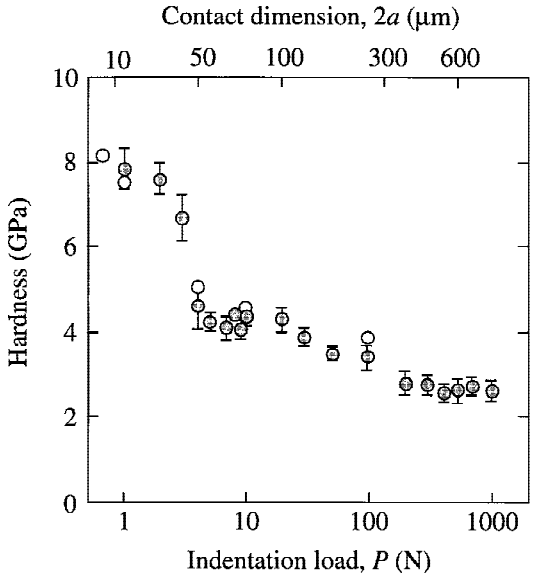

Fig. 1. Vickers hardness (means and standard deviations) as function of indentation load for Ti_3SiC_2. Open circles are data from previous work.[3]

J. E. Ritter—contributing editor

Manuscript No. 190643. Received October 6, 1997; approved November 19, 1997.
Supported by the U.S. Air Force Office of Scientific Research.
[*]Member, American Ceramic Society.
[†]Guest Scientist from the Department of Applied Physics, Curtin University of Technology, Perth WA 6001, Australia.
[‡]Guest Scientist from the Department of Materials Science and Engineering, Lehigh University, Bethlehem, Pennsylvania 18015.

10 mm × 10 mm at a common interface with an intervening thin layer of adhesive, and then polishing the top surface. Indentations were made on the top surface across the surface trace of the bonded interface. The adhesive was then dissolved in acetone, and the top and side surfaces of the separated half-blocks gold coated. Damage zones were observed by optical microscopy in Nomarski illumination and by scanning electron microscopy (SEM).

III. Results

(1) Hardness and Indentation Stress–Strain Curve

Figure 1 plots hardness as a function of indentation load for the Ti_3SiC_2 material. Each data point (mean and standard deviation) was obtained from five measurements. Some data from previous work on similar material are included for comparison.[3] The hardness is highly dependent on the indentation load, falling first abruptly between $P = 1$–5 N and then more gradually at higher loads. This strong dependency of hardness is attributable to the large grain size: when the contact dimension $2a$ of the Vickers impression is less than the grain size (minimum 50 μm), the hardness measures properties of single grains; when $2a$ becomes much larger than the grain size, the hardness measures polycrystalline properties, with more grains oriented for basal slip. The relatively large error bars associated with the data at low loads in Fig. 1 reflect stochastics in the grain orientations in this region.[5]

Figure 2 plots the Hertzian indentation stress–strain curve. The data points are experimental values for the different sphere sizes. The inclined dashed line through the origin is the Hertzian limit for ideal elastic contacts. A yield point $p_Y = 1.0$ GPa representing the contact pressure at first observable deformation is indicated. The data deviate slightly from linearity above this yield point, increasing monotonically with load.[5,6,9]

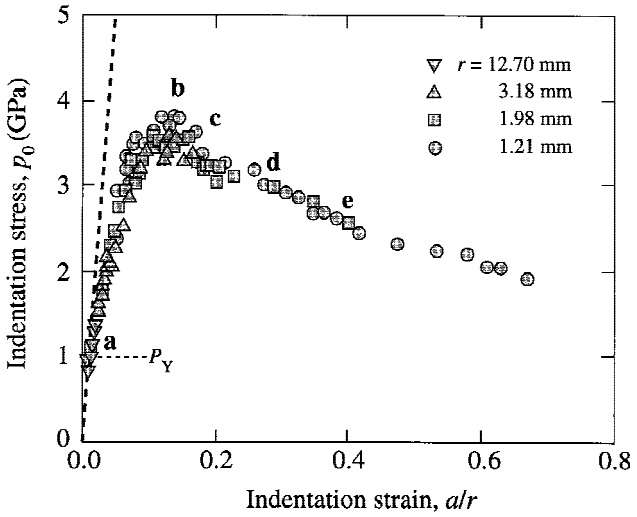

Fig. 2. Indentation stress–strain curve for Ti_3SiC_2. Inclined dashed line is Hertzian elastic response. Labels **a, b, c, d,** and **e** correspond to micrographs in Fig. 3.

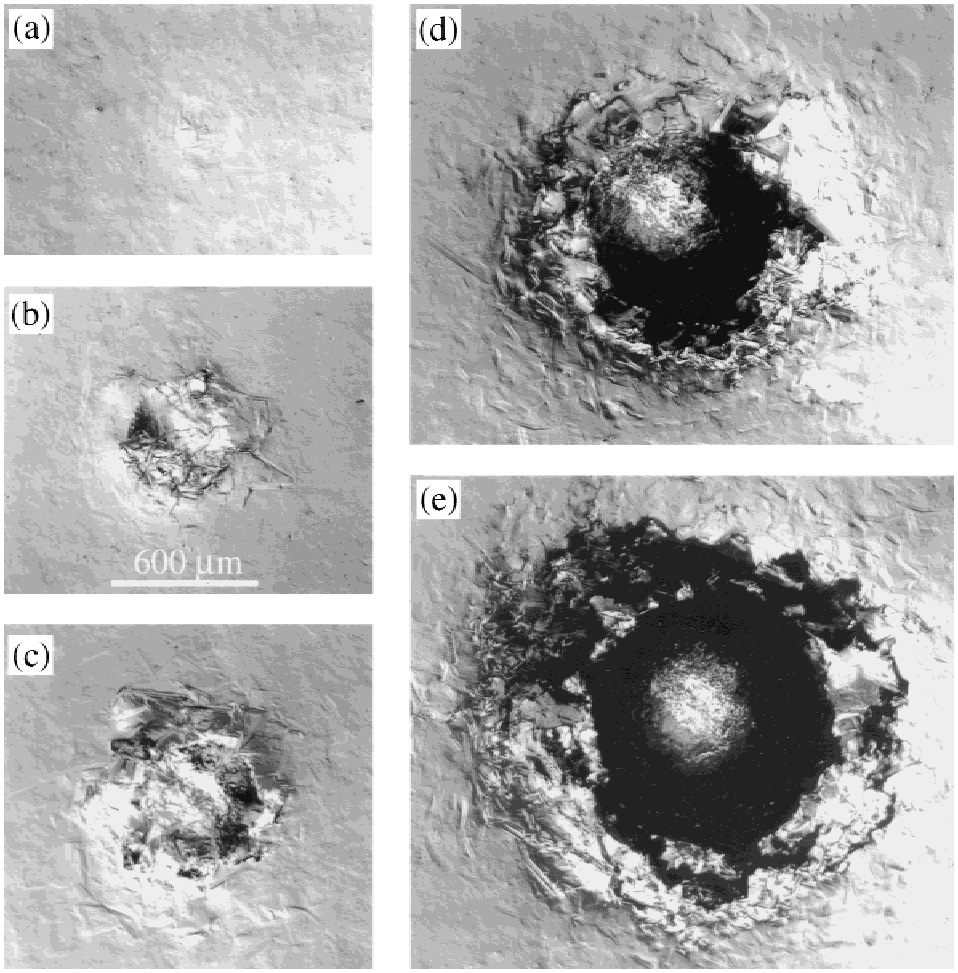

Fig. 3. Surface views of indentation sites in Ti_3SiC_2. Indentations made with WC ball of radius $r = 1.98$ mm. Micrographs (a), (b), (c), (d), and (e) correspond to points labeled in Fig. 2. Optical micrographs, Nomarski illumination.

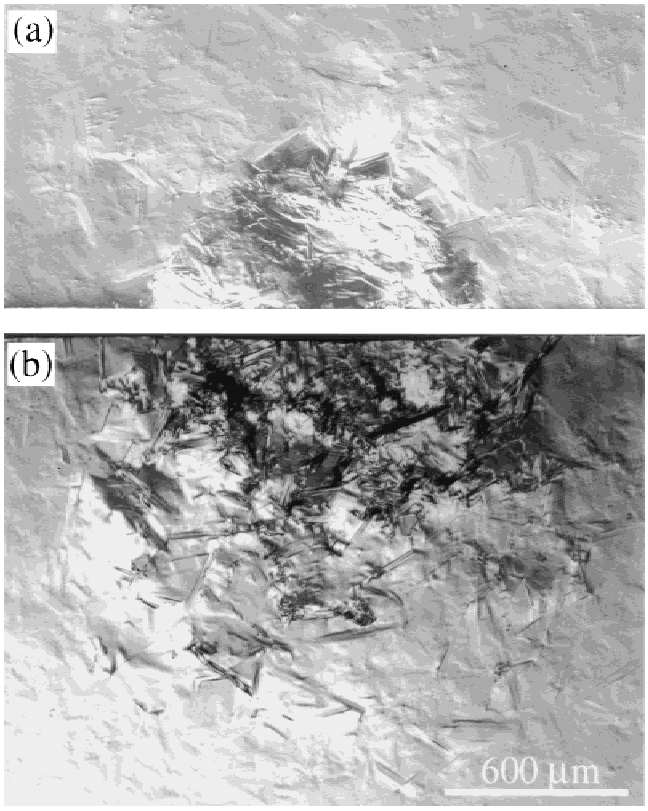

Fig. 4. Half-surface and side view of contact damage from WC ball radius $r = 3.18$ mm at load $P = 2000$ N ($p_0 = 3.6$ GPa). Bonded-interface specimen.

However, the data then pass through a distinctive maximum at $p_0 \approx 3.8$ GPa and thereafter decline steadily in a long tail. This kind of strong strain–softening characteristic is most unusual in ordinarily brittle ceramics, although it is reminiscent of the stress–strain curves observed in rocks in triaxial compression fields.[10]

(2) Contact Damage and Deformation

The optical micrographs in Fig. 3 confirm that the deviation from linearity in the stress–strain curve is due to the onset of indentation damage. The sequence shows surface views of damage for points marked **a, b, c, d,** and **e** in Fig. 2: (a) just above the yield point the first few grains have deformed within the contact area; (b) near the maximum the number of deformed grains within the contact area has markedly increased and individual grain-localized microfaults are observed, typical of tough ceramics;[5,6,9] (c) beyond the maximum stress level the impression is more extensive and deformed grains are observed outside the impression; (d) further along the strain–softening tail the impression is deeper and grain deformation outside the contact area is considerably more pronounced, and material has piled up around the impression; (e) at even higher strain the impression is extensive, and grains beyond the edge of the contact area are heavily deformed, with attendant microcrack coalescence and grain detachment. The complete absence of any ring cracks or cone cracks on the surfaces highlights the predominantly quasi-plastic nature of the damage.

Figure 4 shows a half-surface and section view of the contact damage near the stress–strain maximum (just beyond point **b** in Fig. 2). A distinctive surface depression is observed in the section, attesting to the extent of the deformation. The subsurface deformation is particularly intense, extending well below the contact area. Figure 5 shows optical and SEM micrographs of the center region of the subsurface damage zone in Fig. 4(b). In Fig. 5(a) intralamella slip along basal planes and microfailures along the grain boundaries are evident. In Fig. 5(b) microfailures extend along the grain boundaries intersected by the heavily deformed lamellae, analogous to the generation of microcracks at dislocation pile-ups in metals,[11] and across some of the adjacent grains.

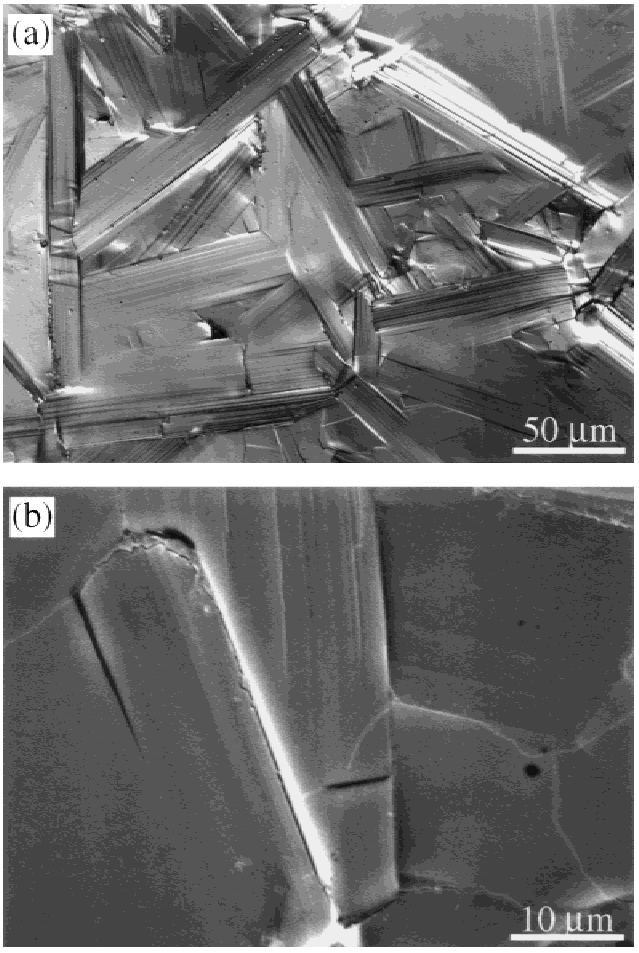

Fig. 5. Micrographs of micromechanical damage from central subsurface region in Fig. 4: (a) optical (Nomarski), (b) SEM.

IV. Discussion

We have investigated contact damage in Ti_3SiC_2 using Hertzian contact. The indentation stress–strain curve in Fig. 2 reveals some distinctive features in the elastic–plastic response. The initial elastic region is steep, commensurate with the high Young's modulus, 320 GPa (a value comparable to that of other hard ceramics like silicon nitride and alumina). The stress–strain curve deviates slightly from linearity above the yield stress, $p_Y = 1.0$ GPa, up to the maximum, $p_0 = 3.8$ GPa. Beyond this point the curve decreases dramatically with increasing strain, indicating strong strain–softening. Such softening behavior is most unusual in ordinarily brittle ceramics (although it is observed commonly in rocks in compression[10]), reflecting the capacity of the material to undergo extensive plastic deformation without macroscopic fracture. The low ratio of hardness/modulus, $H/E = 0.013$, is comparable to soft steel,[4] suggesting an ultimate mechanical behavior more reminiscent of a ductile metal.

There is a microstructural size effect in the Vickers hardness data in Fig. 1.[3] This size effect is associated with the large grain size of the Ti_3SiC_2 material studied here. When the contact area is comparable to the grain size, the contact samples just a few grains—the probability of initiating slip then depends strongly on the local grain orientation. As the contact area increases, more grains are sampled within the near-contact field, and the

likelihood of encountering grains with favorable orientations for deformation is correspondingly higher. Accordingly, the data are subject to greater stochastic variation at low loads,[5] accounting for the larger error bars in this region in Fig. 1.

The micrographs of the damage zones in Figs. 3 and 4 demonstrate extensive shear-driven deformation in the Ti_3SiC_2. The high-magnification micrographs in Fig. 5 reveal the damage to consist predominantly of basal-slip lamellae within grains, with accompanying shear-induced microcracking between grains. The ease and multiplicity of the basal slip process within the individual grains accounts for the exceptional plasticity.[1,3,12] On the other hand, the existence of just one easy slip system precludes a totally plastic response, and ultimately the local strains at the grain boundaries can only be accommodated by the generation of intergranular (or intragranular[3]) microcracks. As these microcracks multiply, extend, and (ultimately) coalesce the modulus of material within the damage zone correspondingly diminishes,[13,14] accounting for the strain–softening seen in Fig. 2.[10] In combination, these easy deformation and microfracture processes at the microstructural level render the material machinable.[1] Other machinable ceramics with platelet structures, e.g., micaceous glass-ceramics (''Macor''),[15] show analogous easy lamella slip, but not to the degree observed in the present material, and without the distinctive strain–softening in the indentation stress–strain curve.[7] The indications are that the present material is somewhat more plastic than the micaceous glass-ceramics, but at the same time still somewhat more brittle than metals with multiple slip systems.

The extreme plasticity of Ti_3SiC_2 lends itself to applications in which high energy absorption with attendant high strains to failure, without microscopic cracking, are a prime requisite. In this sense, Ti_3SiC_2 has the mechanical quality of metals, but still with high elastic rigidity and high-temperature properties characteristic of ceramics. On the other hand, the proliferation of microcracking associated with the quasi-plasticity damage foreshadows some potential limitations, e.g., susceptibility to fatigue[16,17] and low wear resistance.[18]

Acknowledgments: We are grateful to T. El-Raghy for supplying us with specimens for this work. We also wish to thank I. M. Peterson, S. Wuttiphan, Y. G. Jung, and H. Chai for many discussions on experimental aspects of this work.

References

[1]M. W. Barsoum and T. El-Raghy, ''Synthesis and Characterization of a Remarkable Ceramic: Ti_3SiC_2,'' *J. Am. Ceram. Soc.*, **79** [7] 1953–56 (1996).

[2]W. Jeitschko and H. Nowotny, ''Die Kristallstructur von Ti_3SiC_2—Ein Neuer Komplexcarbid-Typ,'' *Monatsh. Chem.*, **98**, 329–37 (1967).

[3]T. El-Raghy, A. Zavaliangos, M. W. Barsoum, and S. R. Kalidindi, ''Damage Mechanisms around Hardness Indentations in Ti_3SiC_2,'' *J. Am. Ceram. Soc.*, **80** [2] 513–16 (1997).

[4]B. R. Lawn and V. R. Howes, ''Elastic Recovery at Hardness Indentations,'' *J. Mater. Sci.*, **16**, 2745–52 (1981).

[5]F. Guiberteau, N. P. Padture, and B. R. Lawn, ''Effect of Grain Size on Hertzian Contact Damage in Alumina,'' *J. Am. Ceram. Soc.*, **77** [7] 1825–31 (1994).

[6]S. K. Lee, S. Wuttiphan, and B. R. Lawn, ''Role of Microstructure in Hertzian Contact Damage in Silicon Nitride: I. Mechanical Characterization,'' *J. Am. Ceram. Soc.*, **80** [9] 2367–81 (1997).

[7]H. Cai, M. A. Stevens Kalceff, and B. R. Lawn, ''Deformation and Fracture of Mica-Containing Glass—Ceramics in Hertzian Contacts,'' *J. Mater. Res.*, **9** [3] 762–70 (1994).

[8]R. M. Davies, ''Determination of Static and Dynamic Yield Stresses Using a Steel Ball,'' *Proc. R. Soc. London*, **A197** [1050] 416–32 (1949).

[9]B. R. Lawn, N. P. Padture, H. Cai, and F. Guiberteu, ''Making Ceramics 'Ductile','' *Science*, **263**, 1114–16 (1994).

[10]J. C. Jaeger and N. G. W. Cook, *Fundamentals of Rock Mechanics;* Ch. 4. Chapman and Hall, London, U.K., 1971.

[11]B. R. Lawn, *Fracture of Brittle Solids;* Ch. 9. Cambridge University Press, Cambridge, U.K., 1993.

[12]B. R. Lawn and D. B. Marshall, ''Nonlinear Stress–Strain Curves for Solids Containing Closed Cracks with Friction,'' *J. Mech. Phys. Solids*, in press.

[13]J. B. Walsh, ''The Effect of Cracks on the Uniaxial Elastic Compression of Rocks,'' *J. Geophys. Res.*, **70** [2] 399–411 (1965).

[14]B. R. Lawn, S. K. Lee, I. M. Peterson, and S. Wuttiphan, ''A Model of Strength Degradation from Hertzian Contact Damage in Tough Ceramics,'' *J. Am. Ceram. Soc.*, in press.

[15]K. Chyung, G. H. Beall, and D. G. Grossman, ''Fluorophlogopite Mica Glass-Ceramics''; pp. 33–40 in Proceedings of the 10th International Glass Congress, No. 14. Edited by M. Kunugi, M. Tashiro, and N. Saga. Ceramic Society of Japan, Kyoto, Tokyo, Japan, 1974.

[16]H. Cai, M. A. S. Kalceff, B. M. Hooks, B. R. Lawn, and K. Chyung, ''Cyclic Fatigue of a Mica-Containing Glass-Ceramic at Hertzian Contacts,'' *J. Mater. Res.*, **9** [10] 2654–61 (1994).

[17]N. P. Padture and B. R. Lawn, ''Contact Fatigue of a Silicon Carbide with a Heterogeneous Grain Structure,'' *J. Am. Ceram. Soc.*, **78** [6] 1431–38 (1995).

[18]V. S. Nagarajan and S. Jahanmir, ''The Relationship between Microstructure and Wear of Mica-Containing Glass-Ceramics,'' *Wear*, **200**, 176–85 (1996). □